Journal of Crystal Growth 644 (2024) 127824

Contents lists available at ScienceDirect

Journal of Crystal Growth

journal homepage: www.elsevier.com/locate/jcrysgro

Explanation for the linear solid/liquid interface recoil observed during directional solidification of a TRIS-NPG alloy under microgravity conditions

A. Ludwig [a,*], J. Mogeritsch [a], H. Barati [b], M. Wu [a], A. Kharicha [a]

[a] Department Metallurgy, University Leoben, Austria
[b] K1-Met, University Leoben, Austria

ARTICLE INFO

Keywords:
A1. Directional solidification
B1. Organic compounds
Alloys

ABSTRACT

During the initial transient stage of a directional alloy solidification experiment, a solid/liquid interface asymptotically recoils from a position that is given by the liquidus temperature to a position given by the solidus temperature. Recent observations onboard the International Space Station revealed that for the organic compound TRIS-NPG, the recoil appears much larger and varies linearly with time. In addition, such conditions were found that the high-temperature non-facetted plastic phase gradually dissolves and, although it seems contradictory to the interpretation of the thermodynamics of the binary system, the low-temperature facetted phase comes into direct contact with the liquid. Both unexpected observations can be understood by assuming that the TRIS-NPG alloy gradually decomposes at the hot side of the furnace. The decomposition products are then transported to the solid/liquid interface by diffusion and the sample motion. The presence of decomposition products changes the binary alloy into a TRIS-NPG-X ternary alloy, with a liquidus temperature that decreases with an increasing amount of decomposed substances.

1. Introduction

The initial transient is the period during directional solidification in which an alloy needs to adapt to the initiation of constant process conditions [1,2]. Hereby, a molten alloy is pulled with a given velocity, V_p, through a constant temperature gradient, G. Under steady-state conditions, if the pulling is not too fast, a planar solid/liquid (s/l) interface solidifies with the same velocity, V, as the pulling speed, V_p. At the s/l interface, solute redistribution occurs according to the phase diagram; its temperature is given by the corresponding solidus temperature T_s. The solute pileup ahead of the front has completely developed, and thus the rate of solute rejection is balanced by the rate of diffusive transport away from the interface. This is the steady-state situation asymptotically reached at the end of the initial transient period.

En route to such steady-state growth conditions, the different solubilities of the liquid and solid lead to a gradual solute pileup ahead of the s/l interface; hence, the interface must recoil from the liquidus T_l to the solidus T_s. When this interface shift is completed, the initial transient ends and steady-state growth follows. The corresponding interface recoil can be approximated by $(T_l\text{-}T_s)/G$ and spans, for the selected model system TRIS-NPG[1] and the applied magnitude of G, over less than a millimetre.

Because products with uniform composition can only be obtained when the initial transient is completed, a quantitative understanding of the initial transient is important in the analysis of many solidification and crystal growth processes. Fabietti et al. [3] demonstrated that to describe the initial transient, it is necessary to account for the gradual increase in the interface velocity. They also demonstrated that in their case, accounting for an initial boundary layer is necessary to determine a correlation between model predictions and experimental findings. Previous models assumed an instantaneously increasing and then constant solidification velocity [4,5], and a uniform composition in the liquid when solidification commences [6–8].

By analysing the s/l interface position during the reduced-gravity directional solidification of a concentrated TRIS-NPG alloy, the authors showed that conditions might exist where the transient build-up of a boundary layer may take much longer than expected [9]. The TRIS-NPG system shows a high-temperature peritectic that involves two

* Corresponding author.
E-mail address: ludwig@unileoben.ac.at (A. Ludwig).

[1] TRIS: tris (hydroxymethyl)aminomethane, NPG: neopentyl glycol.

https://doi.org/10.1016/j.jcrysgro.2024.127824
Received 11 March 2024; Received in revised form 20 July 2024; Accepted 22 July 2024
Available online 23 July 2024

non-facetted, plastic phases [10]. Therefore, it is quite attractive to imitate metal-like solidification phenomena.

The s/l interface recoil measurements that were published in [9] are again shown in Fig. 1. A TRIS-NPG alloy with a nominal composition of $C_0 = 53$ mol% NPG was processed with hot clamps temperatures of $T_{hot} = 439$ K (166 °C) and cold clamps temperatures of $T_{cold} = 379$ K (106 °C). Starting from room temperature, the clamp temperatures of both sides were activated and the position of the solid/liquid interface was measured as soon as the interface was visible ($t = 0$ h in Fig. 1). During the first 8 h, where the cartridge was not pulled, the s/l interface continuously moved towards the cold clamps. During the first 15–30 min it changes fast and during the rest of the 8 h slow. The first rapid motion is caused by the fact that the cartridge with its relatively thick flat fused-silica walls of 2.5 mm and the 1 mm thick NPG-TRIS alloy in between needed time to adapt to the given clamp temperatures (instrumental recoil). The reason for the slower recoil will be discussed later.

The tracers[2] present in the liquid and the small gas bubbles present in the solid also moved during the first 8 h standstill. During the stage that was necessary to thermally equalize the material inside the cartridge, they were both moving toward the cold side of the furnace. This indicates a global movement of the material, probably due to an increasing pressure in the hot part of the cartridge. However, after this initial period, they both moved constantly towards higher temperatures. In ref. [9] it was argued that this might have originated from a still ongoing low-temperature solid/solid phase transition that is known to be quite sluggish. Both phenomena are of minor importance for the current work and are thus ignored in the following.

During the next 8 h, the cartridge was moved with a pulling velocity of $V_p = -0.288$ mm/h. All movements from the hot to the cold clamps are defined here as negative and positive visa verse. Then it was in rest for the next 8 h and then moved again with $V_p = -0.288$ mm/h. Finally, the cartridge was again stopped for the next 4 h. The open and full red dots in Fig. 1 show the measured s/l interface positions. The open red dots are slightly lower than the full red dots because the interface was inclined. The object of the present contribution is to shed light upon the phenomenon that leads to such a large and linearly increasing interface recoil.

2. Numerical procedure

To estimate the diffusion field ahead of a planar s/l interface, three different coordinate systems must be considered: the (non-moving) laboratory system where the temperature distribution between the cold and the hot clamps is given, the first moving system that is fixed with the s/l interface and the second moving system that is fixed with the cartridge. The interrelation between the three coordinate systems is outlined in the Appendix.

To compute and analyse the temperature distribution, a sigmoid function between the hot and the cold zone (Eq. A6) was taken. Evaluating the interface position between the opaque and transparent phases, (O+α versus only α) for several T_{cold} and T_{hot} settings showed that for the present case, the two parameters of the sigmoid function are given as $y_{scale} = 3.2$ mm and $y_{centre} = 1.1$ mm. Fig. 2 shows the corresponding, slightly off-centred temperature and temperature gradient distributions. The dotted line indicates the initial interface position at $y_0^* = 2.05$ mm where the temperature of the solid/liquid interface is supposed to be the liquidus temperature of the alloy. As mentioned in the introduction it takes around 15–30 min until the given clamp temperatures have caused a stable temperature field within the sample material. Within this period, melting at the solid/liquid interface continued and the interface position moved to the corresponding liquidus temperature. This is known as instrumental recoil. After this initial period, the interface position changed its dynamics, as can be seen in Fig. 1. For the remaining of the first 8 h standstill, the interface continued to gradually move towards the cold clamps with an almost constant velocity. The origin of this motion will be discussed later. The initial interface position at $y_0^* = 2.05$ mm is de facto a result of extrapolating the interface position of the remaining first 8 h standstill $t_o = 0$ h. The corresponding interface temperature is approximately $T_0^* = 413$ K which corresponds to an alloy composition of $C_0 = 48$ mol% NPG rather than the nominal 53 mol%. The reason for this discrepancy is that during leak testing on Earth, the cartridge was melted and resolidified in an upright standing position. This created a creeping buoyancy flow that brought lighter NPG-rich liquid to the top of the cartridge and thus led to a composition reduction at the bottom; the part that is located on the hot side.

Fig. 3 shows the liquidus and solidus temperatures for the metastable α-phase in the high NPG region, T_l and T_s, as well as the corresponding curves for the redistribution coefficient, k, and the liquidus slope, m, as suggested in [10]. Note that for the simulation of the interface recoil as presented in the next section, m is not needed as $T_l(C)$ is directly used.

For modelling the recoil curve, as measured for TAC4S3 (Fig. 1), the following three stages are to be distinguished: (i) a fine-grained microstructure in a given temperature gradient during the first 8 h; (ii) growth of an inclined but otherwise planar s/l interface; and (iii) melting (negative growth) of that s/l interface at the end of the second and third standstill periods.

During the first stage, bubbles and tracers indicated that the material within the cartridge had moved at a speed of approximately $V = 0.016$ mm/h towards the hot zone. This was unexpected and could be triggered by two different volume-increasing effects, namely the slow transformation of the faceted NPG phase into the plastic phase at the cold clamps temperature, and the density adjustment of the plastic phase within the temperature gradient itself. As the s/l interface consisted of fine grains, they were pushed to higher temperatures where they melted. This process did not change the concentration at the s/l interface. The observed grain boundary migration via Temperature Gradient Zone Melting (TGZM) is of greater importance [10–12]. This phenomenon transports segregated intergranular liquid to the s/l interface and thus increases the mean concentration at the interface. In [9] it was speculated that this process might explain the interface recoil during the first standstill period. In what follows, we will demonstrate that another phenomenon might be more important to explain the results from our observations.

The second and the third stages were modelled by considering (i) the sample pulling, (ii) planar solidification/melting by accounting for the NPG flux balance at the s/l interface, and (iii) diffusion of NPG along the solute gradient that forms on building up/removal of the solute pileup ahead of the s/l interface. An effect of the latent heat on the temperature gradient was neglected as the growth velocity was extremely small. Further details on the modelling approach are given in the Appendix.

3. Results and discussion

It is the properitectic α-phase that forms the s/l interface recoiling as shown in Fig. 1. This was justified in [9]. Fig. 4 shows the numerically estimated interface recoil for five different diffusion coefficients, D, considering α-growth and applying $T^* = T_l$, k, and m, as a function of the interfacial liquid concentration, C_l^*, as given in [10]. The reason for testing a variety of diffusion coefficients is that doubts about the exact value of D are appropriate. In his Ph.D. thesis [13], one of the authors (JM) estimated values of D as a function of TRIS-NPG composition by using the TGZM method. Values between $D = 1.1{\cdot}10^{-11}$ m^2/s = 0.04 mm^2/h and $3{\cdot}10^{-11}$ m^2/s = 0.11 mm^2/h were suggested. However, as outlined in [10] for non-dilute alloys, the assumption of a concentration-independent diffusion coefficient that is valid for the entire droplet

[2] The tracers are probably dirt particles that were undesirably present in the sample material.

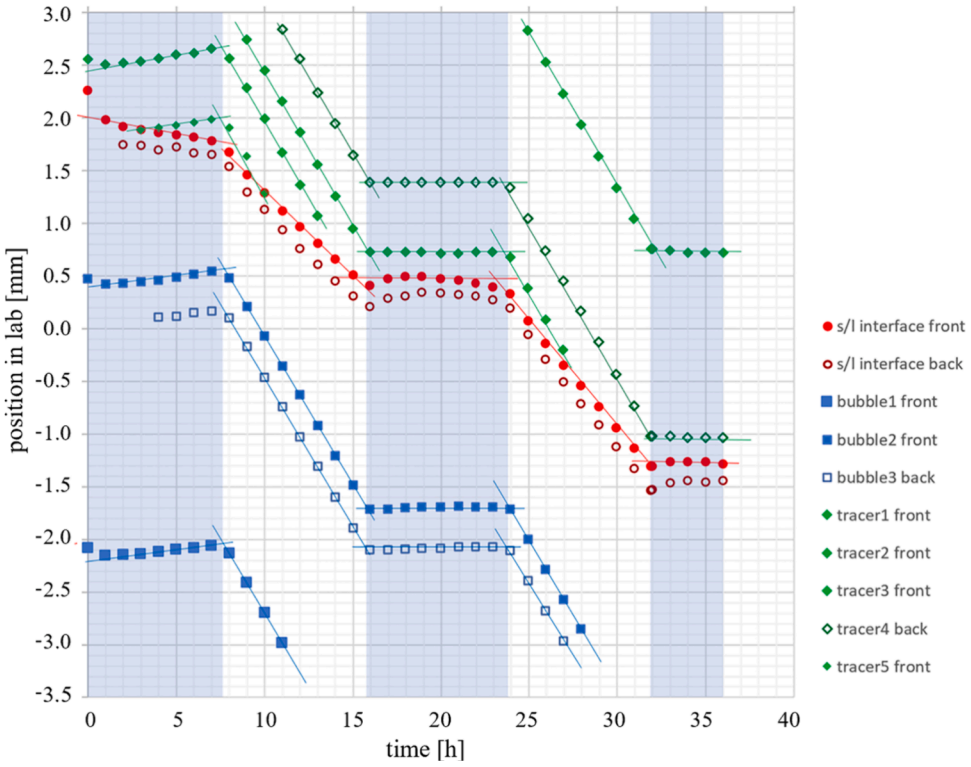

Fig. 1. Measured s/l interface recoil as reported in ref. [9].(The measurements were taken during the METCOMP-TAC4S3 campaign processed between April 20, 2021, 18:32 GMT, and 22 April 22, 2022, 06:37 GMT on the International Space Station, ISS.) Blue-shaded regions represent periods of standstill, white regions those of sample pulling with V_p = -0.08 µm/s = -0.288 mm/h. The nominal alloy concentration was C_0 = 53 mol% NPG. Measurements were done with the focus of the objective lens at the front and back windows of the cartridge. The positions are measured in a laboratory frame of reference with the origin at the centre of the observation window and the positive axis pointing towards the 'hot' side. (For interpretation of the references to colour in this figure legend, the reader is referred to the web version of this article.)

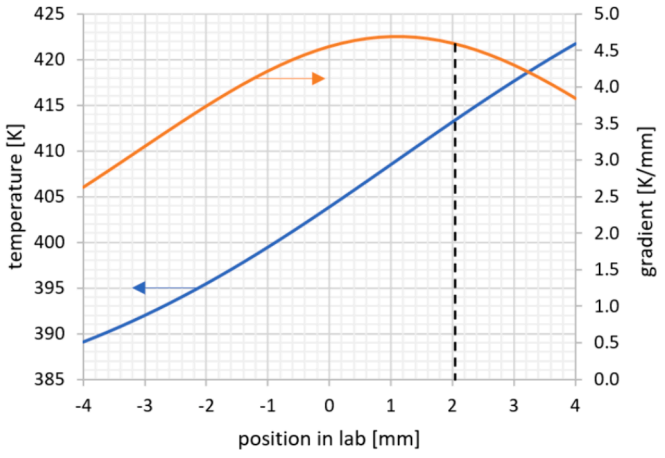

Fig. 2. Assumed temperature distribution between the cold and hot zones. The blue curve shows the temperature and the orange one the temperature gradient. The zero point of the laboratory coordinate system is located in the centre of the observation window that spans from −3.05 mm to +3.05 mm. The starting position of the experiment TAC4S3 is indicated by the dotted line: 2.05 mm measured from the centre of the observation window and 1 mm from its right side. (For interpretation of the references to colour in this figure legend, the reader is referred to the web version of this article.)

TGZM trajectory is vague. The dotted lines in Fig. 4 approximately indicate the experimental interface position at the end of each standstill period. During the first 8 h standstill, melting of the fine-grained microstructure is modelled by assuming $k = 1$, and the effect of TGZM on the interface concentration is ignored. Thus, the interface does not change position. Naturally, the smaller the D value, the faster the interface tends to reach the position of the solidus temperature as solute can be effectively accumulated ahead of the interface. This explains why the curves with a smaller D are above those with a larger D. After 8 h of pulling, a solute pileup has established ahead of the s/l interface. However, only for D = 0.04 mm^2/h, the NPG concentration at the interface accumulates in such a manner that the nominal solidus temperature is reached in less than 8 h. With $T_l - T_s$ = 3.2 K and G = 4.6 K/mm, the expected interface recoil for getting into steady-state is 0.7 mm. That is the value estimated in Fig. 4 for the curve D = 0.04 mm^2/h. For all the other diffusion coefficients, 8 h pulling is not enough to reach steady-state conditions. During the succeeding 8 h of standstill, the solute pileup gradually dissipates, and thus the interface concentration drops and the interface temperature increases again. Similar processes occur during the second pulling and standstill stages. Note that for D = 0.04 mm^2/h the 8 h standstill is not sufficient to completely counterbalance the solute pileup that had formed during 8 h pulling. Thus, the interface has to grow into a non-uniform solute distribution during the second 8 h growth. This causes the local minimum of the corresponding D = 0.04 mm^2/h curve. Comparing these curves with the one presented in Fig. 1, it is obvious that they cannot reproduce the measured interface recoil.

One argument that could explain this discrepancy might be the presence of unintended impurities. An impurity may act as a further alloying element that changes the solidification path and leads to a reduction of the final temperature for complete solidification. Like the NPG, the impurities would also accumulate ahead of the growing s/l interface, and, after stopping to pull the sample, dissipate into the bulk melt. So, the recoiling curves for α-growth with accounting for impurities would principally resemble the ones shown in Fig. 4 except that they reach lower interface positions. In particular, at the end of the

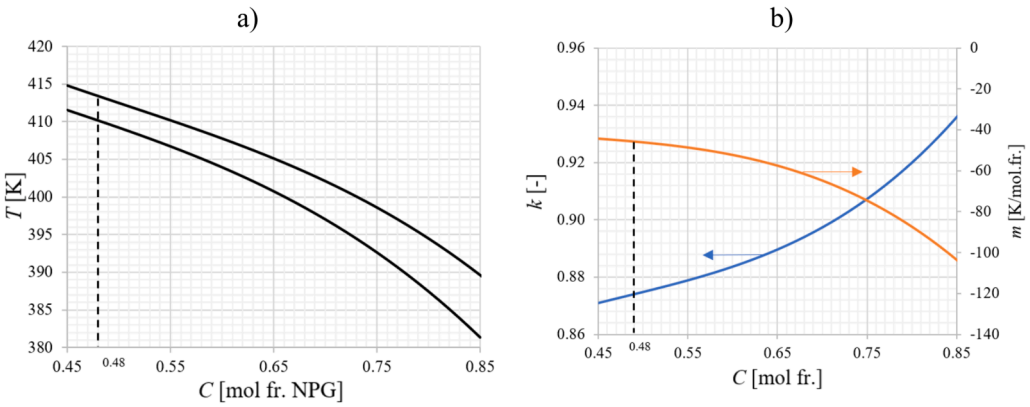

Fig. 3. a) Liquidus and solidus temperatures for the metastable pro-peritectic α-phase in the high NPG-rich region as suggested by [10]. b) Corresponding functions of the redistribution coefficient, *k*, in blue and liquidus slope, *m*, in orange. In the Appendix, all shown graphs are given as polynomial functions of alloy concentration, *C*. (For interpretation of the references to colour in this figure legend, the reader is referred to the web version of this article.)

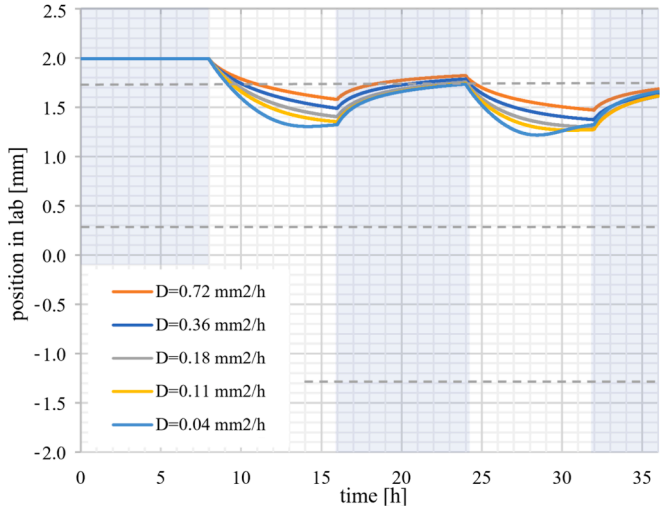

Fig. 4. Simulated interface recoil considering thermodynamic principles as given in [10] for the pro-peritectic α-phase and solute diffusion ahead of the s/l interface. The dotted lines indicate approximately the experimental interface positions at the end of each standstill period.

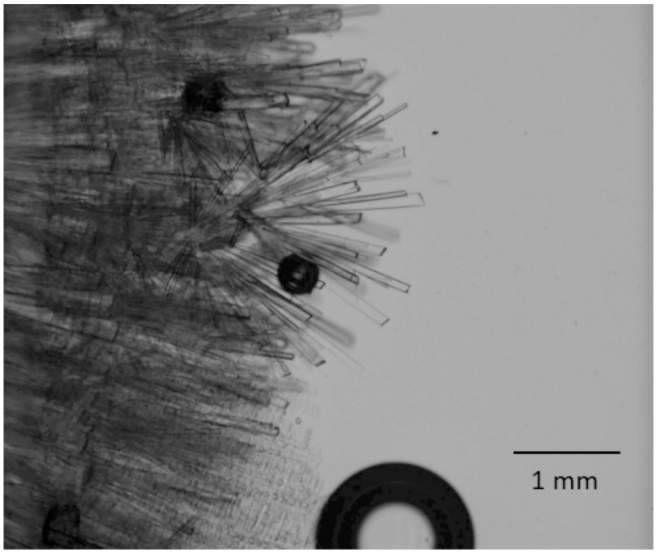

Fig. 5. Facetted needle crystals in contact with the liquid in the upper part of the image and melting dendritic structures from the plastic α-crystal in the lower part. The right side was exposed to the hot temperature clamps, and the left side to the cold ones. At the time when the image was taken the corresponding cartridge section had been processed under various conditions for approximately 60 h (2.5 h at 130/130 °C, 1 h at 101/161 °C, 24 h at 96/156 °C with V_p = -0.05 μm/s, 7 h at 91/151 °C with V_p = 0 μm/s, 7 h at 85/146 °C with V_p = 0 μm/s, 13 h at 81/141 °C with V_p = -0.05 μm/s, 7 h at 81/141 °C with V_p = 0 μm/s.). The nominal alloy composition was C_0 = 51 mol% NPG. (The image was taken from the 2023 μg-campaign of TAC1S5 recorded on 12. Oct. 2023, 01:50:06 GMT at the ISS.).

second standstill period, the corresponding recoiling curves would display the same asymptotic behaviour as diffusion will also counterbalance the solute pileup of the unintended impurities. This contradicts the measurements as during the last three hours of the second standstill period the interface position in the experiment gradually decreases again, indicating melting! (Fig. 1).

In [9] it was speculated that the increasing interface positions at the end of the second standstill period might be caused by an NPG enrichment via grain boundary TGZM. Although some grain boundaries appeared during the second standstill, they were rare and hardly visible. The situation is completely different compared to the first standstill where fine grains coarsened and grain boundaries migrate via TGZM. The experimentally observed decreasing interface position at the end of the second standstill period must therefore be originated by something else.

During the 2023 μg-campaign onboard the International Space Station (ISS) with TRIS-NPG samples, conditions occurred that showed the low-temperature facetted O-phase in direct contact with the liquid (Fig. 5). The high-temperature plastic α phase had nearly completely disappeared. This observation contradicts the phase diagram, even the metastable one that disregards the peritectic β-phase and that predicts that the α-phase forms a solid solution over the full concentration range of TRIS-NPG [10]. It is that observation which led us to conduct further investigations on a previously conducted long-term experiment.

In [10], we have reported an experiment with TRIS-NPG (C_0 = 50 mol% NPG) in a stationary temperature gradient, where the focus had been on how the microstructure reacts to changing thermal conditions. Starting with the s/l interface position shown in Fig. 3c2 of ref. [10], the interface position was now further evaluated over an additional period of more than 20 h. Although the thermal conditions during this period had been kept constant and only a few grain boundaries were present, the s/l interface further recoiled by approximately 0.56 mm. Obviously, the pro-peritectic α-phase disappears over time when being kept immobile in a stationary temperature gradient.

To understand this observation, it is paramount to explain that liquid TRIS-NPG alloys at elevated temperatures gain a brown tinge with time;

the higher the temperature, the faster this happens. Knowing that, for the μg-campaign using TRIS-NPG alloys for solidification experiments it was decided that the hot clamps' temperature should not exceed 170 °C and the maximum processing time should be under 36 h. For the experiment of Fig. 1 the hot clamps temperatures were set to 166 °C and the processing time to indeed 36 h. Based on the extreme recoiling behaviour unveiled by comparing Figs. 1 and 4, a thermal decomposition/degradation of most probably the TRIS molecules at the hot clamps area must be considered.

Thermal decomposition is often described by a kinetic model [14]. The most often used equation is of Arrhenius type as

$$\frac{\partial f_\varphi}{\partial t} = A\exp\left(-\frac{E_a}{RT}\right)(1-f_\varphi)^n \tag{1}$$

with f_φ being the volume fraction of decomposition products. A, E_a and R are the Arrhenius preexponential factor, the apparent activation energy, and the gas constant, respectively. The expression $(1-f_\varphi)^n$ is the so-called kinetic model function, which describes variation in the reaction rate as the reaction proceeds at a constant temperature. Various expressions for this function are given in [14]. Unfortunately, the authors are not aware of the relevant parameters for TRIS (or NPG). However, for HMX[3] it was reported that the time for 10 % decomposition varies from 830 h at 120 °C to 3 s at 260 °C [15]. That is an enormous time difference that might be typical for HMX. However, for TRIS (or NPG) at $T_{\text{hot}} = 439$ K (166 °C), it cannot be ruled out that the thermal decomposition might have already started although full decomposition might take days or even weeks. As we have found Peritectic Couple Growth (PCG) in TRIS-NPG at compositions where this growth form was expected [16,17], it can be stated that the impact of the thermal decomposition of the TRIS (or NPG) molecules on the occurring solidification morphologies is small, at least for the first day of processing. Nevertheless, the unusual recoil behaviour led us to reconsider how important thermal decomposition might be for the present experiment.

Thermal decomposition studies are usually done by applying calorimetry, thermogravimetry and mass spectrometry. Examples of such investigations can be found in [18] for several ethanolamines (mono-, di-, tri-, methyldi-) and in [19] for several amino acids. Especially for the amino acids, thermal decomposition happens at temperatures where gaseous NH_4 and H_2O dissociate from the compound. A similar process is conceivable for TRIS with $C_4H_{11}NO_3 \rightarrow NH_4 + 3{\cdot}H_2O{+}C_4H_2$,[4] as we have observed an increasing amount of bubbles in processed TRIS-NPG samples.

Naturally, the formation rate of decomposition products in the hot zone area is higher compared to the region close to the s/l interface. Although it is not yet known exactly what types of decomposition products emerge, it is suggested to describe their presence by one decomposition product concentration, C_φ. The exact profile of the C_φ ahead of the s/l interface depends on (i) the thermal decomposition, (ii) C_φ diffusion, (iii) motion of the cartridge (convection), and (iv) the redistribution coefficient of the decomposition product(s) at the s/l interface. At the beginning of the experiment, C_φ is zero everywhere. Over time C_φ increases according to Eq. (1) at a maximum rate in the hot zone area. Thus, a C_φ gradient forms with a slowly rising C_φ^* at the s/l interface and a more rapidly rising C_φ at the hot zone. Without any sample motion, this gradient will continue to become steeper, although diffusion acts to equalize C_φ. With pulling, two additional phenomena are also increasing C_φ^*, sample pulling (convection) and solute redistribution at the growing s/l interface. Especially if the decomposition product(s) are not incorporated into the solid, they will pile up ahead of the front and, with time, the corresponding concentration profile might change from simply increasing, to first decreasing and then increasing, so that a local minimum at some distance from the interface forms. The exact shape of the corresponding C_φ profile could be estimated by a 1D diffusion simulation if the following five parameters for the decomposition product(s) are known: redistribution coefficient, diffusion coefficient, Arrhenius preexponential factor, Arrhenius activation energy, and Arrhenius exponent for the kinetic model function. As all five parameters are basically unknown, we have abstained from performing such 1D diffusion simulations.

In the binary TRIS-NPG system, the interface temperature, T^*, is related to the NPG composition at the liquid side of the interface, C_l^*, by the relation, $T^*(C_l^*)$ (Eq. A8). If the thermodynamics now change to become a TRIS-NPG-X ternary system, T^* will also depend on C_φ^*. The simplest function to account for that is

$$T^*(C^*, C_\varphi^*) = T^*(C^*) - m_\varphi C_\varphi^* \tag{2}$$

with a liquidus surface slope m_φ in the direction of C_φ and the unaffected binary relation $T^*(C_l^*)$. Both, m_φ and C_φ^* are *a priori* unknown. In the following, we assume that C_φ^* increases linearly in time,

$$C_\varphi^*(t) = \mathrm{X}_{np}t - \mathrm{X}_p V_p t \tag{3}$$

with X_{np} and X_p being unknown parameters. The first term accounts for the formation of decomposition products at the interface, the impact of diffusion and the impact of solute rejection at the moving (growing/melting) interface and the second term for cartridge pulling. Note that $V_p < 0$ for pulling from hot to cold. Inserting Eq. (3) in Eq. (2) it becomes obvious that the unknown parameters are de facto, $m_\varphi \mathrm{X}_{np}$ and $m_\varphi \mathrm{X}_p$. They can be estimated to best reproduce the measurements.

The first term in Eq. (3) is justified by the fact that the formation of C_φ^* by decomposition can be approximated with a function that is linear in time, as long as there is just a small fraction of decomposition products ($f_\varphi^* \ll 1$). For accounting for the impact of diffusion, we have tried to use a 'square-root-of-t' term rather than a linear one. However, the best reproduction of the measurements was obtained with the suggested linear term. Obviously, decomposition is more important than diffusion. The increase of C_φ^* by cartridge pulling depends on the pulling velocity, V_p and is represented by the second term in Eq. (3). However, a linear increase is only obtained when C_φ in front of the s/l interface also increases linearly. A decreasing C_φ profile with a local minimum at some distance from the s/l interface would lead to a C_φ^* decrease on pulling. The measurements do not suggest that. Obviously, the C_φ pileup ahead of the s/l interface due to solute rejection is small compared to the C_φ increase in thermal decomposition.

As shown in Fig. 1, the interface position changes approximately from 2.0 to 1.7 mm during the first 8 h standstill. According to Fig. 2, this corresponds to a T^* reduction of approximately 1.2 K. Hence, we obtain $m_\varphi \mathrm{X}_{np} = 0.15$ K/h. For the second parameter, we have tested different values and found that with $m_\varphi \mathrm{X}_p = 2$ K/mm the experimental measurements can be reproduced with ease. Fig. 6 shows the estimated recoil curves for the different coefficients of NPG diffusion. At least for the larger D values, the interface at the end of the second standstill recoils as also noticeable in the experiment. Following the present argumentation, we conclude that this behaviour is due to the ongoing decomposition of the organic compound at the s/l interface.

Although the simulated recoil curves resemble those that were measured, there are admittedly several open issues that may lead to doubts about the quantitative comparison. For example, the assumption that the decomposition does not have an effect on the partitioning of NPG at the s/l interface is rather crude. Therefore, the only statement that can be taken seriously is that the interface temperature gradually decreases until the α-phase solid fully disappears and that the presence

[3] HMX: 1,3,5,7-tetranitro-1,3,5,7-tetrazocane.
[4] C_4H_2 is known as Propalene.

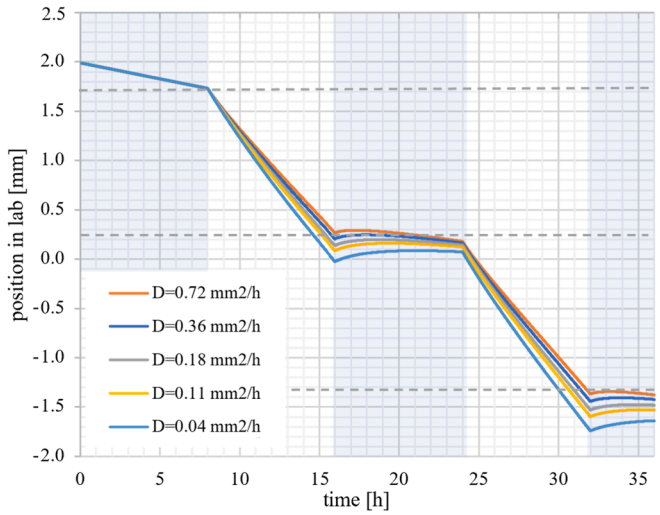

Fig. 6. Simulated interface recoil considering both diffusion-driven growth of the pro-peritectic α-phase and a T_l−reduction according to Eq. (2)-(3). The following parameters were used: $m_\varphi X_{np} = 0.15$ K/h and $m_\varphi X_p = 2$ K/mm.

of decomposition products at the s/l interface is certainly a good indicator to explain this finding.

4. Conclusions

Decomposition in the area surrounding the hot clamps of most probably TRIS (but also NPG) is crucial to understand the observed linear interface recoil during the initial transient stage of peritectic (or near-peritectic) TRIS-NPG alloys. As the decomposition rate depends on the temperature, the amount of decomposition products decreases with increasing distance from the hot clamps area. Therefore, a gradient of decomposition products must be assumed in front of the s/l interface that further steepens with time. During sample pulling, the decomposition products are then transported towards the interface. With the assumption that the decomposition products change the characteristics of the alloy so that the binary TRIS-NPG system changes into a ternary TRIS-NPG-X alloy, it is natural that the liquidus temperature drops with an increasing amount of decomposition products. This liquidus temperature reduction continues until the high-temperature non-facetted plastic phase completely disappears and the low-temperature facetted phase comes into direct contact with the liquid.

Due to a lack of essential data, accurate numerical modelling of this process is far not possible. For now, no information on the decomposition kinetics for the TRIS and the NPG molecules is available. However, the extremely unusual linear interface recoil during the initial transient of peritectic (and near-peritectic) TRIS-NPG alloys, as well as the dissolution of the high-temperature non-facetted α-phase can be logically explained, and, with some empirical parameters, also quantitatively described by assuming the decomposition of the organic compound.

CRediT authorship contribution statement

A. Ludwig: Writing – review & editing, Writing – original draft, Supervision, Conceptualization. **J. Mogeritsch:** Investigation. **H. Barati:** Software. **M. Wu:** Validation. **A. Kharicha:** Validation.

Declaration of competing interest

The authors declare the following financial interests/personal relationships which may be considered as potential competing interests: Prof. Andreas Ludwig reports financial support was provided by Austrian Research Promotion Agency. If there are other authors, they declare that they have no known competing financial interests or personal relationships that could have appeared to influence the work reported in this paper.

Data availability

No data was used for the research described in the article.

Appendix

Initial Transient formulation

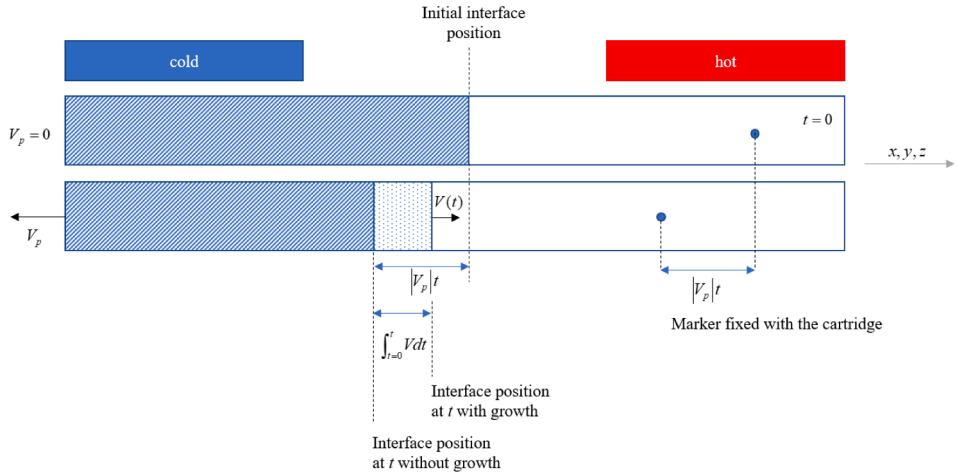

Fig. A1. Schematic drawing that illustrates planar growth during the initial transient.

Let us consider the withdrawal of a long sample with a constant pulling velocity $V_p < 0$ and a planar s/l interface that solidifies with a (changing) growth velocity $V > 0$ in a temperature gradient G. V_p points in the opposite direction compared to V and therefore it is taken negative. The diffusion

field ahead of the planar s/l interface can be estimated in three reference frames: (i) specimen (x,t); (ii) laboratory (y,t); and (iii) s/l interface (z,t). It is considered that the three coordinate systems are initially coincident and the interface is located at $x^* = y^* = z^* = 0$. The diffusion equation in the **specimen frame of reference** is

$$\frac{\partial C}{\partial t} = \frac{\partial}{\partial x}\left[D\frac{\partial C}{\partial x}\right] \tag{A1}$$

where the s/l interface changes position accordingly to $x^* = \int_{t=0}^{t} V dt$. The diffusion equation in the **laboratory frame of reference** is as follows:

$$\frac{\partial C}{\partial t} = V_p\frac{\partial C}{\partial y} + \frac{\partial}{\partial y}\left[D\frac{\partial C}{\partial y}\right] \tag{A2}$$

where the s/l interface is located at $y^* = \int_{t=0}^{t} V dt + V_p t$. The diffusion equation in the **s/l interface frame of reference** is

$$\frac{\partial C}{\partial t} = -V\frac{\partial C}{\partial z} + \frac{\partial}{\partial z}\left[D\frac{\partial C}{\partial z}\right] \tag{A3}$$

where the s/l interface is located at $z^* \equiv 0$. Eq. (A3) indicates that the s/l interface frame of reference changed from the laboratory frame of reference at $V = 0$ (start of pulling) to the specimen frame of reference at $V = -V_p$ (steady state). The corresponding coordinate transformations are given by:

$$y = x + V_p t, z = x - \int_{t=0}^{t} V dt \text{ and } z = y - V_p t - \int_{t=0}^{t} V dt \tag{A4}$$

The boundary condition at the s/l interface is independent of the frame of reference and is given by

$$VC^*(1-k) = D\frac{\partial C^*}{\partial x} = D\frac{\partial C^*}{\partial y} = D\frac{\partial C^*}{\partial z} \tag{A5}$$

Generally, the redistribution coefficient k and the liquidus slope m are functions of the concentration C. Thus, in Eq. (A5), k must be evaluated as $k = k(C_l^*)$, and later, in Eq. (A8), m as $m = m(C_l^*)$.

The temperature T and temperature gradient G are given by the experimental conditions in the **laboratory frame of reference**, $T = T(y)$, and $G = G(y)$, and can be expressed using a sigmoid function as

$$T(y) = T_{\text{cold}} + S(y)(T_{\text{hot}} - T_{\text{cold}}) \text{ with } S(y) = \frac{1}{1+e^{-\chi(y)}} \text{ and } \chi = \frac{y - y_{\text{centre}}}{y_{\text{scale}}} \tag{A6}$$

and

$$G(y) = S'(y)(T_{\text{hot}} - T_{\text{cold}}) = S(y)(1-S(y))\chi'(y)(T_{\text{hot}} - T_{\text{cold}}) \tag{A7}$$

The concentration at the interface, C^*, is related to the liquidus temperature based on the phase diagram. For the pro-peritectic α-phase in the TRIS-NPG phase diagram, we obtain a third-order polynomial for the liquidus temperature

$T_l(C) = a_3C^3 + a_2C^2 + a_1C + a_0$ with $a_0 = 457.27$ K,

$$a_1 = -175.58 \text{ K/(mol fr.)}, a_2 = 256.21 \text{ K/(mol fr.)}^2, \text{ and } a_3 = -168.57 \text{ K/(mol fr.)}^3, \tag{A8}$$

the redistribution coefficient

$k(C) = a_{k3}C^3 + a_{k2}C^2 + a_{k1}C + a_{k0}$ with $a_{k0} = 0.7622$,

$$a_{k1} = 0.5409, a_{k2} = -0.9677, \text{ and } a_{k3} = 0.6723, \tag{A9}$$

and the liquidus slope

$m(C) = a_{m3}C^3 + a_{m2}C^2 + a_{m1}C + a_{m0}$ with $a_{m0} = 17.595$ K/mol fr.,

$$a_{m1} = 366.23\text{K/(mol fr.)}, a_{m2} = 783.01 \text{ K/(mol fr.)}^2, \text{and } a_{m3} = -611.29\text{K/(mol fr.)}^3. \tag{A10}$$

Applying Eq. (A8) with the actual interface concentration and using the reverse of Eq. (A6) (the so-called logit function) yields the corresponding interface position in the **laboratory frame of reference** as

$$y^* = \chi^* y_{\text{scale}} + y_{\text{centre}} \text{ with } \chi^* = \chi(y^*) = \ln\frac{S(y^*)}{1-S(y^*)} \text{ and } S(y^*) = \frac{T_l(C^*) - T_{\text{cold}}}{T_{\text{hot}} - T_{\text{cold}}} \tag{A11}$$

The corresponding change of Δy^* is related to the actual growth velocity by $V = \Delta y^*/\Delta t + V_p$ (see Eq. (A2)). Note that Δy^* is negative during the initial transient, and thus, $V < V_p$.

Numerics

Assuming a 1D grid consisting of non-uniform intervals Δz and a diffusion coefficient that does not vary along z, Eq. (A3) in its implicit finite-difference version is given by

$$\frac{C-C_{old}}{\Delta t} = -V\frac{C_{next}-C_{prev}}{\left(\Delta z_{prev}+\Delta z_{next}\right)} + D\frac{\frac{C_{next}-C}{\Delta z_{next}} - \frac{C-C_{prev}}{\Delta z_{prev}}}{1/2\left(\Delta z_{prev}+\Delta z_{next}\right)}. \tag{A12}$$

Here, C_{next} is the concentration of the right neighbouring node of C with distance Δz_{next}, and C_{prev} is the concentration of the left neighbouring node with distance Δz_{prev}. With some modifications, Eq. (A12) can be rewritten as:

$$aC = bC_{next} + cC_{prev} + C_{old}$$

with $a = 1 + q_2 + q_3$, $b = q_1 + q_2$, $c = -q_1 + q_3$

and

$$q_1 = -\frac{V\Delta t}{(\Delta z_{prev}+\Delta z_{next})}, q_2 = \frac{2D\Delta t}{(\Delta z_{prev}+\Delta z_{next})\Delta z_{next}}, q_3 = \frac{2D\Delta t}{(\Delta z_{prev}+\Delta z_{next})\Delta z_{prev}} \tag{A13}$$

For the boundary condition Eq. (A5), Eq. (A13) yields that

$$C^* = C_1 = \frac{DC_2}{D - V(1-k)(z_2 - z_1)} \tag{A14}$$

where the growth velocity must be iteratively determined to fulfil $T_l(C^*) = T(y^*)$ together with $V = \Delta x^*/\Delta t = \Delta y^*/\Delta t - V_p$.

References

[1] W. Kurz, D.J. Fisher, Fundamental of Solidification, 4th ed., Trans. Tech. Publ., Aedermansdorf, 1998. doi: 10.4028/www.scientific.net/RC.35.

[2] J.A. Dantzig, M. Rappaz, Solidification, 2nd ed., EPFL Press, 2016.

[3] L.M. Fabietti, P. Mazumder, R. Trivedi, Dynamics of planar interface growth during directional solidification of alloys, Scr. Mater. 97 (2015) 29–32, https://doi.org/10.1016/j.scriptamat.2014.10.019.

[4] W.A. Tiller, K.A. Jackson, J.W. Rutter, B. Chalmers, The redistribution of solute atoms during the solidification of metals, Acta Met. 1 (1953) 428–437, https://doi.org/10.1016/0001-6160(53)90126-6.

[5] V.G. Smith, W.A. Tiller, J.W. Rutter, A Mathematical Analysis of Solute Redistribution During Solidification, Can. J. Phys. 33 (1955) 723–745, https://doi.org/10.1139/p55-089.

[6] B. Caroli, C. Caroli, L. Ramirez-Piscina, Initial front transients in directional solidification of thin samples of dilute alloys, J. Cryst. Growth. 132 (1993) 377–388, https://doi.org/10.1016/0022-0248(93)90062-2.

[7] J.A. Warren, J.S. Langer, Prediction of dendritic spacings in a directional-solidification experiment, Phys. Rev. E 47 (1993) 2702–2712, https://doi.org/10.1103/PhysRevE.47.2702.

[8] S.R. Coriell, R.F. Boisvert, G.B. McFadden, L.N. Brush, J.J. Favier, Morphological stability of a binary alloy during directional solidification: initial transient, J. Cryst. Growth. 140 (1994) 139–147, https://doi.org/10.1016/0022-0248(94)90507-X.

[9] A. Ludwig, J. Mogeritsch, M. Rettenmayr, On/off directional solidification of near peritectic TRIS-NPG with a planar but tilted solid/liquid interface under microgravity conditions, Scr. Mater. 214 (2022) 114683, https://doi.org/10.1016/j.scriptamat.2022.114683.

[10] A. Ludwig, J. Mogeritsch, V.T. Witusiewicz, Hypo-peritectic TRIS–NPG in a Stationary Temperature Gradient: Thermodynamics, Grain Boundary Migration and Phase Identification, J Cryst. Growth. 604 (2023) 127052, https://doi.org/10.1016/j.jcrysgro.2022.127052.

[11] W.G. Pfann, Temperature gradient zone melting, AIME. 203 (1955) 961–964, https://doi.org/10.1007/BF03377594.

[12] W.A. Tiller, Migration of a liquid zone through a solid, J. Appl. Phys. 34 (1963) 2757–2769, https://doi.org/10.1063/1.1729806.

[13] J. Mogeritsch, Investigation on peritectic solidification using a transparent organic system, Ph.D. Thesis, Montanuniversitaet Leoben, AUT, 2012.

[14] N. Koga, S. Vyazovkin, A.K. Burnham, L. Favergeon, N.V. Muravyev, L.A. Pérez-Maqueda, C. Saggese, P.E. Sánchez-Jiménez, ICTAC Kinetics Committee recommendations for analysis of thermal decomposition kinetics, Thermochim. Acta. 719 (2023), https://doi.org/10.1016/j.tca.2022.179384.

[15] A. Burnham, R. Weese, Thermal decomposition kinetics of HMX, Lawrence Livermore National Lab., Livermore, CA, United States, 2004. doi: 10.2172/877784.

[16] A. Ludwig, J. Mogeritsch, In Situ Study of Peritectic Couple Growth Under Purely Diffusive Conditions, Met. Mater. Trans. A 54 (2023) 4179–4187, https://doi.org/10.1007/s11661-023-07052-6.

[17] A. Ludwig, J. Mogeritsch, Observations of the occurrence and disappearance of peritectic couple growth performed under microgravity conditions, Scr. Mater. 239 (2024) 115802, https://doi.org/10.1016/j.scriptamat.2023.115802.

[18] S.G. de Ávila, M.A. Logli, J.R. Matos, Kinetic study of the thermal decomposition of monoethanolamine (MEA), diethanolamine (DEA), triethanolamine (TEA) and methyldiethanolamine (MDEA), Int. J. Greenh. Gas Control. 42 (2015) 666–671, https://doi.org/10.1016/j.ijggc.2015.10.001.

[19] I.M. Weiss, C. Muth, R. Drumm, H.O.K. Kirchner, Thermal decomposition of the amino acids glycine, cysteine, aspartic acid, asparagine, glutamic acid, glutamine, arginine and histidine, BMC Biophys. 11 (2018) 1–15, https://doi.org/10.1186/s13628-018-0042-4.